An Experimental Study on Dynamic Mechanical Properties of Fiber-Reinforced Concrete under Different Strain Rates

Yuexiu Wu [1], Wanpeng Song [2,3,*], Wusheng Zhao [3,*] and Xianjun Tan [3,*]

[1] Key Laboratory of Rock Mechanics in Hydraulic Structural Engineering, Ministry of Education, Wuhan University, Wuhan 430072, China; yuexiuwu@whu.edu.cn

[2] Engineering Technology Research Institute of CCTEB Group Co., Ltd., Wuhan 430064, China

[3] State Key Laboratory of Geomechanics and Geotechnical Engineering, Institute of Rock and Soil Mechanics, Chinese Academy of Sciences, Wuhan 430071, China

[*] Correspondence: songwanpeng555@163.com (W.S.); wszhao@whrsm.ac.cn (W.Z.); xjtan@whrsm.ac.cn (X.T.); Tel.: +86-13349913380 (W.S.); +86-15872386874 (W.Z.); +86-15972092588 (X.T.)

check for updates

Abstract: Fiber-reinforced concrete (FRC) has a great advantage in earthquake-resistant structures, as compared with regular concrete. However, there are many difficulties in the construction and maintenance of concrete structures due to the high density and easy corrosion of the steel fiber in commonly used steel FRC. With the development of polymer material science, polyvinyl alcohol (PVA) fiber has been rapidly promoted for use in FRC because of its low density, high strength, and large elongation at break value. Dynamic uniaxial compression and splitting tensile experiments of FRC with PVA fiber were carried out with two matrix strengths (i.e., C30 and C40), which were blended with PVA fibers with a length of 12 mm in different volume contents (0, 0.2, 0.4, and 0.6%), at the age of 28 days, under different strain rates (i.e., 10^{-5}, 10^{-4}, 10^{-3}, and 10^{-2} s^{-1}). The results show that PVA has an obvious enhancing and toughening effect on concrete, which can improve its brittle properties and residual strength. With increasing strain rate, the compressive strength, split tensile strength, and elastic modulus increase to a certain extent, while the toughness index and the peak strain decrease to a certain degree. The post-peak deformation characteristic changes from a brittle failure of sudden caving to a ductile failure with dense cracking. The effect of PVA is different when enhancing the concrete with two different matrix strengths. The lower the matrix strength, the more obvious the enhancement effect of the fiber, showing characteristics of a higher compressive strength and low split tensile strength in FRC with low strength and a smoother post-peak stress–strain curve.

Keywords: seismic load; strain rate; fiber-reinforced concrete; dynamic mechanical property

1. Introduction

Concrete is a porous, brittle material widely used in civil engineering. It has a high compressive strength but poor tensile strength, impact resistance, and toughness, which results in a weak resistance to cyclic, impact, seismic, and explosive loads. Therefore, many scholars have been exploring ways to improve the tensile performance of concrete. One of the most promising methods of modification is to add an appropriate amount of chaotic fibers to plain concrete, which can improve the tensile strength, stiffness, fatigue life, and ductility of the concrete, based on the influence of the fiber on the initial crack initiation and propagation [1–3]. There are a wide variety of fibers that can be used for the reinforcement of concrete—i.e., metallic fibers, organic fibers, and inorganic fibers—according to material composition. These fibers mainly include steel fiber, glass fiber, polypropylene fiber, polyvinyl

alcohol (PVA) fiber, basalt fiber, and coir fiber [4,5]. Presently, there are many studies on the enhancing and toughening effect of fiber-reinforced concrete (FRC) under static loads. Song and Hwang [6] studied the characteristics of the compressive strength, split tensile strength, and fracture modulus of concrete with different steel fiber contents. It was found that compressive strength was the highest with a fiber content of 1.5%, and the split strength, toughness index, and fracture modulus increased with increasing fiber content. Yazici et al. [7] studied the characteristics of compressive strength, split tensile strength, flexural strength, and ultrasonic velocity of steel FRC with different aspect ratios and volume contents. Some conclusions have also been drawn, that the addition of steel fiber could significantly improve the split and bending strength, while the improvement in compressive strength was not obvious and ultrasonic velocity showed a downward trend. Vajje and Krishnamurthy [8] focused on the characteristics of natural fiber concrete with different types of fibers, including basalt fiber, jute, sisal, hemp, banana, and pineapple. The results showed that the properties of FRC were related to the material properties of the fiber itself. There are also many studies on natural fiber concrete, which show that the addition of natural fibers results in a certain degree of improvement in the split tensile strength, bending strength, and absorbing energy of the concrete, with the fiber content in concrete relating to the fiber type [9–11]. Shafiq et al. [12] carried out a three-point bending experiment on PVA and basalt FRC beams with different contents (1–3%). The results showed that PVA fibers could significantly improve the post-peak bending behavior of concrete beams compared with basalt fiber. The PVA concrete beams showed deflection hardening characteristics with 3% content, while the basalt fiber concrete beams showed deflection softening characteristics with high content. However, the diameter of the PVA fiber (0.66 mm) was larger than that of the basalt fiber (0.018 mm). The different bending properties of FRC beams should have a certain relationship with fiber diameter.

From the above studies, it is evident there have been many achievements in testing fiber concrete with different kinds of fiber under static loads. However, concrete is a brittle material with a high sensitivity to strain rate [13,14]. Concrete structures will inevitably encounter a variety of dynamic loads during their service period, such as the wind load suffered by ground constructions and bridges, the hydrodynamic pressure encountered by dams and maritime terminals, and the seismic loads encountered by engineering structures in strong earthquake areas. Many studies have shown that the properties of concrete under a dynamic load are quite different from those under a static load. Therefore, it must be irrational to use the concrete strength parameters under static loads to design concrete structures that may be subjected to dynamic loads during service. It is important to study the strength and deformation characteristics of concrete or fiber concrete under dynamic loads. According to the existing research results [4,15], the strain rate of a concrete structure under different loads can be further divided into the following types: creep load (10^{-8}–10^{-6} s^{-1}), static load (10^{-6}–10^{-5} s^{-1}), vehicle load (10^{-5}–10^{-4} s^{-1}), seismic load (10^{-4}–10^{-2} s^{-1}), impact load (10^{-2}–10^2 s^{-1}), and explosion and high-speed collision load (10^2–10^4 s^{-1}). Abrams et al. [16] first carried out the compression experiments of concrete under static load (with a strain rate of approximately 8×10^{-6} s^{-1}) and dynamic load (with a strain rate of ~2×10^{-4} s^{-1}) and found that there was a strain rate sensitivity for the compressive strength of concrete. In 1917, many scholars carried out a variety of dynamic experimental studies on the mechanical properties of concrete and FRC. Cook et al. [17] used the drop hammer experimental system to study the dynamic mechanical properties of coir FRC and found that the impact index of fiber concrete increased with the increase of fiber length and content. Zhang et al. [18] conducted three-point bending tests on notched beams of steel FRC under a large range of loading rates by using both a servo-hydraulic machine (with a loading rate of ~10^{-3}–1 mm/s) and a drop-weight impact device (with a loading rate of approximately 10^2–10^3 mm/s). The experimental results showed that the rupture energy and the peak load increased with increasing loading rate, and the growth values at a low loading rate were smaller than those at a high loading rate. This was due to the viscous effects of free water at lower rates and the inertia effect and greater fiber pullout energy at high rates. Dong et al. [1] studied the mechanical properties of basalt fiber-reinforced recycled aggregate under different replacement ratios and contents of basalt fiber (e.g., concrete failure modes,

compressive strength, tensile strength, elastic modulus, Poisson's ratio, and ultimate strain under static conditions) and some mechanical properties under cyclic loading and unloading. The experimental results showed that the basalt fiber enhanced the mechanical properties of recycled aggregate concrete.

Currently, the most commonly used fibers in concrete are steel fibers, which have significantly improved the tensile properties of concrete. However, the addition of steel fiber not only improves the tensile strength, but also increases the weight of the concrete structure [19]. The development of polymer materials science has led to the fabrication of the newly developed PVA, which is a kind of synthetic fiber with a low price, high strength, and high elastic modulus. It has good hydrophilicity and a high bonding strength with cementitious material. This not only effectively inhibits early cracks in the concrete, but also improves the strength, toughness, and durability of the concrete [20]. At present, the enhancing properties of PVA have been confirmed in the application of Engineered Cementitious Composite (ECC) concrete, which does not contain coarse aggregate [21–23]. However, due to the large content of PVA in concrete (2%) without coarse aggregate, the cost of concrete is so high that the application is still limited to the key parts of structures subjected to large forces in engineering. This is not conducive to large-scale promotion of PVA fiber concrete. Now, the available dynamic characteristics of PVA FRC with coarse aggregate also concentrate on high strain rates, such as impact loads, explosions, and high-speed collision loads. There are still few studies on the dynamic characteristics at the strain rate of seismic loads for fine PVA FRC that are suitable for testing the strength of an engineering structure.

Strong earthquake activity has brought huge losses to the western region of infrastructure construction in China, which is an earthquake-prone country. Due to the poor tensile properties of conventional concrete, the traditional support structures are prone to drawing, bending, and shearing under the action of a seismic load, so it is necessary to develop high tensile performance in an underground structure to reduce damage taken in strong earthquake areas. This is of great significance for the design of concrete structures. In this paper, the dynamic experiments of PVA concrete, with two matrix strengths designed for the engineering of structures, are carried out to study the strengthening and toughening effect of PVA in different contents under quasi-static state and dynamic loads, which will be useful for the application of FRC in earthquake prone areas.

2. The Sample Preparation for the FRC with PVA

2.1. Experimental Materials and Production

2.1.1. PVA Fiber

The experimental fiber is the TQ-II -II type of hardened anti-cracking synthetic fiber. The fibers are bunched monofilament, white, safe, and non-toxic. The detailed parameters and actual picture are shown in Table 1 and Figure 1, respectively. According to the test report by the National Textile and Garment Quality Supervision Inspection Center (Zhejiang) (No. 201509666 document), the measured mechanical indicators of PVA used in the experiment meet industry requirements. The specific test results are shown in Table 2.

Table 1. Physical and mechanical parameters of polyvinyl alcohol (PVA) fiber.

Fiber Shape	Density (g/cm^3)	Fiber Diameter (μm)	Fiber Length (mm)	Tensile Strength (MPa)	Elastic Modulus (GPa)	Elongation at Break (%)	Acid and Alkali Resistance
Bunchy monofilament	1.30	15–25	12	≥1200	≥30	5–20	Strong

Table 2. Test report results of PVA fiber.

Serials No.	Test Items	Standard Requirement	Measured Value	Individual Assessment
1	Tensile strength (MPa)	≥1200	1721.2	Qualified
2	Initial elastic modulus (GPa)	≥30	35.7	Qualified
3	Elongation at break (%)	5–20	7.0	Qualified

Figure 1. Image of PVA.

2.1.2. Mixture Design Proportions and Mixing of FRC

The mix design is in accordance with the Chinese standards outlined in "Specification for mix proportion design of ordinary concrete" (JGJ55-2011) [24] and "Steel fiber-reinforced concrete" (JG/T 472-2015) [25]. After several adaptations and experiments, concrete with two matrix strengths (i.e., C30 and C40) with different fiber contents was designed. The specific design parameters are shown in Table 3. In the table, the types of concrete are named after two matrix strengths and different fiber contents. For example, C40PVA0.4 indicates that the matrix strength was 40 MPa and the volume content of PVA was 0.4%. In order to minimize the effect of the coarse aggregate and fine aggregate on the experimental results, the difference between the two contents was made to be small, and the sand ratio was fixed at 35%. The water/cement ratios for the two matrix strengths concrete were designed to maintain a constant of 0.53 and 0.49, respectively, so as to reduce the effect of water/cement on the experimental results.

Table 3. Mix proportions of fiber-reinforced concrete (FRC) (1 m^3).

Type	Cement (kg)	Water (kg)	Fine Aggregate (kg)	Coarse Aggregate (kg)	W/C	Sand Ratio	PVA Volume Content
C30PVA0	377.6	200	643.1	1194.3	0.53	35%	0%
C30PVA0.2	377.6	200	643.1	1194.3	0.53	35%	0.2%
C30PVA0.4	377.6	200	643.1	1194.3	0.53	35%	0.4%
C30PVA0.6	377.6	200	643.1	1194.3	0.53	35%	0.6%
C40PVA0	438.8	215	611.17	1135.03	0.49	35%	0%
C40PVA0.2	438.8	215	611.17	1135.03	0.49	35%	0.2%
C40PVA0.4	438.8	215	611.17	1135.03	0.49	35%	0.4%
C40PVA0.6	438.8	215	611.17	1135.03	0.49	35%	0.6%

It has been found that the key factor in the success of the experiment is the dispersion of the fiber in concrete during the process of multiple adaptation of the fiber concrete. According to the relevant

research, we can see that the smaller-diameter fiber is less likely to be dispersed in the concrete; hence, the amount of fine fibers in concrete should not exceed a certain number. Based on a number of mixing experiments and the mixing experience of fiber concrete outlined in the literature, a fast and efficient laboratory mixing method is put forward. First, an appropriate amount of coarse aggregate and fine aggregate is put into the forced mixer machine to dry mix for 30 s, and the PVA fiber and cement is put into the pot to dry mix for 2 min. Then, the fiber and cement mixture are placed in the forced mixer to dry mix with the coarse aggregate and fine aggregate mixture until the cement and fiber are mixed evenly, and the designated water quantity is added for wet mixing for 3 min. After the above process is complete, the fiber will be distributed evenly in the mixed FRC without the occurrence of the knot phenomena, meeting construction requirements. The specific construction process is illustrated in Figure 2.
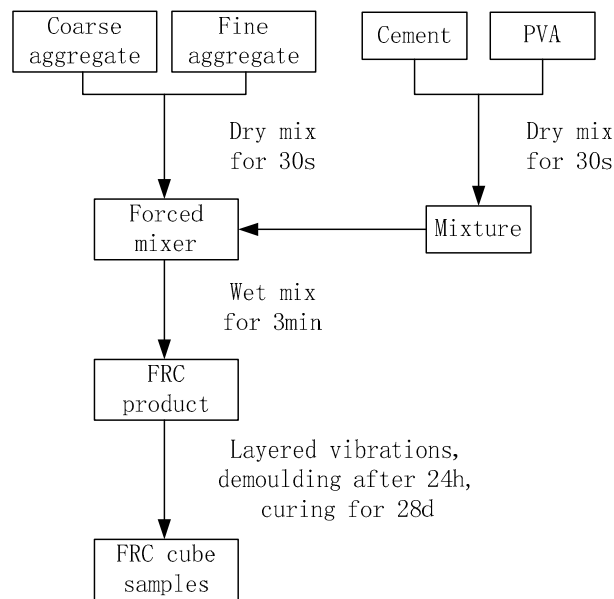
Figure 2. Flow chart for FRC mixing and pouring.

The mixed fiber concrete is placed in a standard plastic sample mold, with dimensions of 150 × 150 × 150 mm, in three layers and vibrated for 2 min. Then, it is covered with cling film to prevent moisture from evaporating. After 24 h, the samples need to be demolded and put into the standard curing room for water conservation at a temperature of 20 ± 2 °C and a humidity greater than or equal to 95%. After curing for 28 days, the samples are ready for the relevant mechanical experiments.

2.2. Experimental Program

The dynamic compression and splitting tensile mechanics experiment of fiber concrete under a medium strain rate were carried out by using the RMT-201 rock and concrete mechanics experiment system developed by the Wuhan Institute of Rock and Soil Science at the Chinese Academy of Sciences. In the experiment, a 150 × 150 × 150 mm plastic mold was used to cast the concrete, and samples of the two kinds with different sizes were prepared by drilling from the mold. The experiment was carried out with four kinds of fiber volume contents (i.e., 0, 0.2, 0.4, and 0.6%) and four different strain rates (i.e., 10^{-5}, 10^{-4}, 10^{-3}, and 10^{-2} s^{-1}). The dynamic compression experiments were conducted with a cylindrical sample with the size of Φ50 × 100 mm, 3 samples per group, and a total of 48 samples. The sample for the dynamic splitting experiment was a cylinder sample with a size of Φ50 × 30 mm. There were 3 samples per group, and a total of 48 samples. The total number of dynamic experiments was 192, with two different sizes for two matrix strengths of concrete.

3. Experimental Results and Discussion

3.1. Compression Strength

The experimental results of the compressive strength for FRC at different strain rates are shown in Figures 3 and 4. In general, the compressive strength of FRC increases with the increase of strain rate, showing an obvious rate sensitivity, which agrees with the existing research [13,14,16–18]. At the quasi-static strain rate (i.e., a strain rate of 10^{-5} s^{-1}), the strength of the two kinds of plain concrete meet the design requirements. The addition of PVA can lead to an increase in compressive strength with the two matrix strengths. Under the quasi-static state, the maximum growth values for the FRC of C30 and C40 are 15.1% and 8.7%, respectively, relative to the two types of plain concrete. With the increase of strain rate, there is a significant difference in the increase of the compressive strength with different fiber volume contents. The two types of concrete with a fiber content of 0.2% show the maximum growth at different strain rates, which is related to the most uniform distribution of PVA fibers in concrete, similar to previous findings [6].
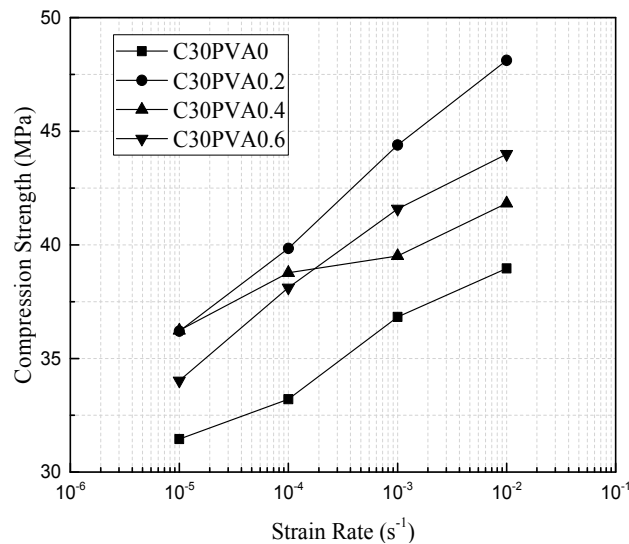
Figure 3. Uniaxial compressive strength of FRC (C30).
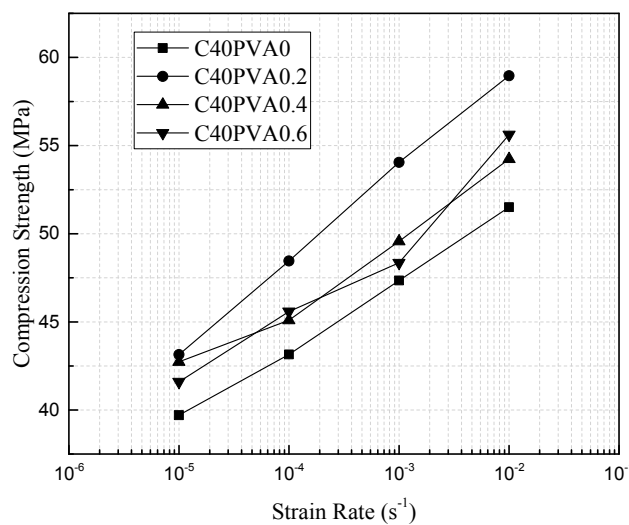
Figure 4. The uniaxial compressive strength of FRC (C40).

From the experimental results, it can be seen that the matrix strength of concrete is another important factor that affects the compressive strength of FRC, in addition to fiber volume content and

loading rate. The higher the matrix strength of the concrete, the smaller the effect of PVA on the increase in compressive strength, which is consistent with experimental results from literature [18,26]. Taking the FRC with a volume content of 0.2% as an example, the growth values of uniaxial compressive strength for a matrix strength of C30 are 15.1, 20.9, 20.6, and 23.5%, respectively for each strain rate tested compared with plain concrete at the same strain rates. For C40, the values are 8.7, 12.3, 14.2, and 8.1% for each strain rate, respectively, which are significantly lower than those of C30. The reason for this phenomenon is related to the bond strength and the matrix strength between the fiber and the concrete [1]. Under the same conditions, the reinforcing effect of the fiber is constant. The higher the matrix strength, the lower the proportion of the fiber reinforcement in the high strength concrete. This, in turn, will weaken the fiber-reinforcing effect.

In order to describe the dynamic strength characteristics of FRC under different loading rates, a series of empirical formulas are proposed, including a logarithmic function [27], exponential function [28], and Fib model code [29], which have many practical applications. In the uniaxial compression experiment, as the reinforcing effect of the concrete with 0.2% content is the best, the empirical formula of dynamic compressive strength with different matrix strengths is established by fitting the relevant experimental data for the FRC with 0.2% PVA content. The fitting dynamic impact factor formulas and the fitting curves are shown below, as in Figure 5. The fitting results clearly confirm the above conclusions that the higher the matrix strength, the weaker the fiber-reinforcing effect.

$$DIF_c = \frac{f_c}{f_{cs}} = 1.1591 + 0.0258 \lg\left(\frac{\dot{\varepsilon}}{\dot{\varepsilon}_s}\right) \text{ for C30PVA0.2} \tag{1}$$

$$DIF_c = \frac{f_c}{f_{cs}} = 1.0951 + 0.0193 \lg\left(\frac{\dot{\varepsilon}}{\dot{\varepsilon}_s}\right) \text{ for C40PVA0.2} \tag{2}$$

where DIF_c, f_c, f_{cs}, $\dot{\varepsilon}$, and $\dot{\varepsilon}_s$ are the dynamic impact factor of compression strength, dynamic compression strength, quasi-static compressive strength, dynamic strain rate, and quasi-static compression strength, respectively.
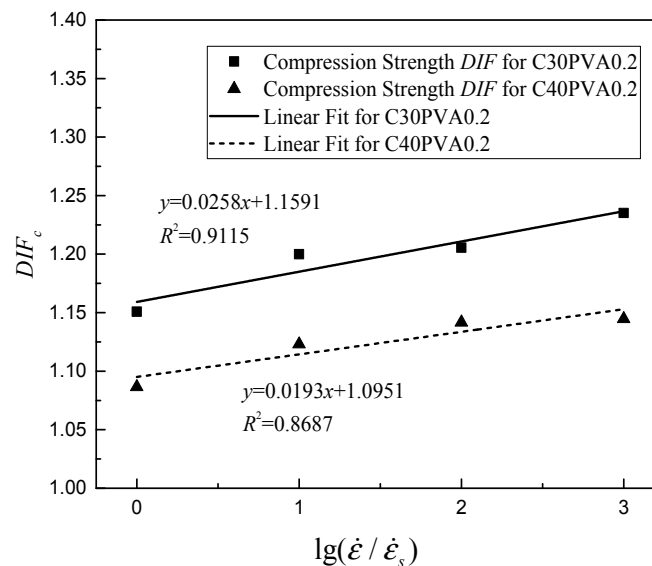
Figure 5. Fitting curves of compressive strength DIF_c for C30PVA0.2 and C40PVA0.2.

3.2. Split Tensile Strength

The experimental results of the split tensile strength of fiber concrete at different strain rates are shown in Figures 6 and 7. Similar to the law of the compressive strength, the addition of PVA can also increase the tensile strength of concrete. In the quasi-static state (i.e., a strain rate of 10^{-5} s^{-1}), the addition of PVA significantly improved the tensile strength of FRC compared with plain concrete,

as also seen in previous findings [28]. When the matrix strength of concrete is C30, the growth values are 19.4, 10.9, and 20.3% for fiber volume contents of 0.2, 0.4, and 0.6%, respectively. When it is C40, the growth values are 17, 10.9, and 7%, respectively. The tensile strength of FRC also has a rate sensitivity compared with plain concrete. As strain rate increased, the splitting tensile strength with different contents increased to some extent, while the growth rate increased first and then decreased later, which did not follow the law of the compressive strength. In the low range of strain rates (e.g., 10^{-5} and 10^{-4} s^{-1}), the bridging effect of the fiber plays a major role in concrete. At this time, the increase of the tensile strength of fiber concrete depends mainly on the bonding force between the fiber and the cementitious material. As the strain rate increases (e.g., to 10^{-3} or 10^{-2} s^{-1}), the increase of the loading rate exceeds the expansion rate of the cracks inside the concrete. Hence, the concrete aggregate is directly cut off, and the bridging effect of the fiber is relatively weakened, resulting in the tensile strength of FRC showing a downward trend, as compared with that of plain concrete. In general, the bridging effect of the fiber plays a major role at low strain rates. With the increase of strain rate, the bridging effect of the fiber is weakened, leading to the change of the concrete fracture form from the destruction of cementitious material under a low strain rate to the direct cut of coarse aggregate a under high strain rate. This is confirmed in the existing literature [30,31] and shown in Figure 8.
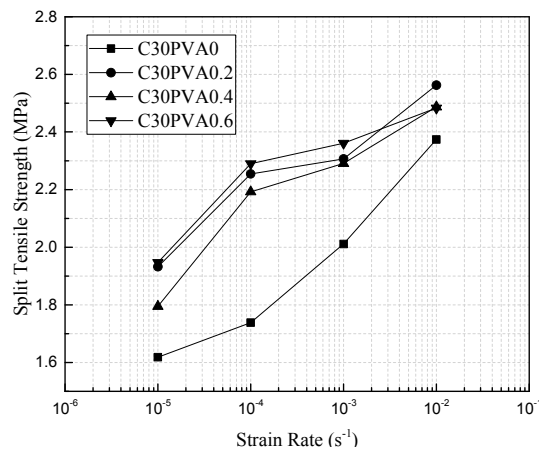
Figure 6. Split tensile strength of FRC (C30).
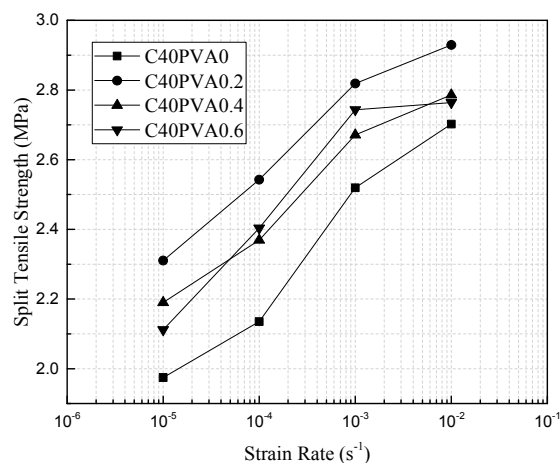
Figure 7. Split tensile strength of FRC (C40).
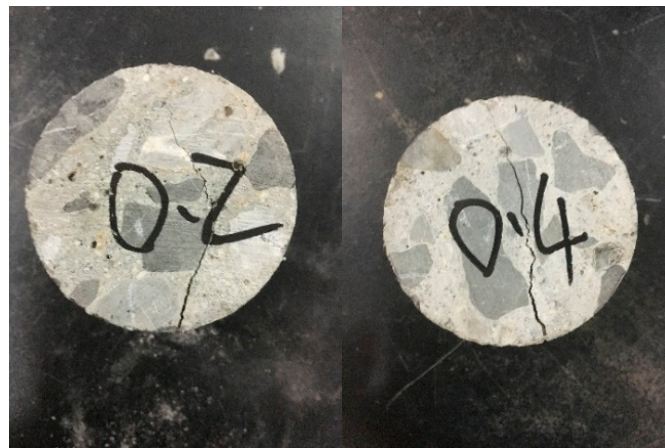
Figure 8. Two kinds of split tensile failure modes of FRC.

According to the fitting method of the dynamic impact factor in the concrete compression experiment, the formula for the dynamic tensile strength of fiber concrete with 0.2% content is established by using polynomial fitting. The fitting formula and curves are shown below, as in Figure 9. From the fitting results, the conclusion that a higher matrix strength is directly related to weaker fiber enhancement is equally applicable to splitting tensile strength. However, unlike the fitting curves of compressive strength, the curves of splitting tensile strength tend to increase first and then decrease. The dynamic impact factor of split tensile strength of fiber concrete reaches the maximum at a strain rate of 10^{-4} s^{-1} for both matrix strengths.

$$DIF_t = \frac{f_t}{f_{ts}} = 1.211 + 0.0783 \lg\left(\frac{\dot{\varepsilon}}{\dot{\varepsilon}_s}\right) - 0.0426\left[\lg\left(\frac{\dot{\varepsilon}}{\dot{\varepsilon}_s}\right)\right]^2 \text{ for C30PVA0.2} \tag{3}$$

$$DIF_t = \frac{f_t}{f_{ts}} = 1.1766 + 0.0087 \lg\left(\frac{\dot{\varepsilon}}{\dot{\varepsilon}_s}\right) - 0.0139\left[\lg\left(\frac{\dot{\varepsilon}}{\dot{\varepsilon}_s}\right)\right]^2 \text{ for C40PVA0.2} \tag{4}$$

where DIF_t, f_t, and f_{ts} are the dynamic impact factor of split tensile strength, dynamic split tensile strength, and quasi-static split tensile strength, respectively. $\dot{\varepsilon}$ and $\dot{\varepsilon}_s$ have the same meaning as previously described above.
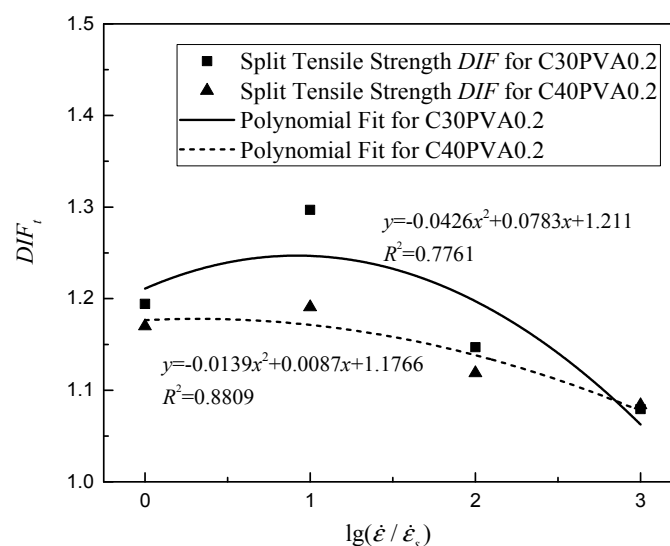
Figure 9. Fitting curves of split tensile strength DIF_t for C30PVA0.2 and C40PVA0.2.

3.3. Elastic Modulus and Peak Strain

The elastic modulus of FRC at different strain rates is shown in Figures 10 and 11. The results show that the elastic modulus of FRC increases with the increase in the strain rate, similar to the compressive strength and split tensile strength [1,7,18,26]. The increasing range of the elastic modulus is different in FRC with different matrix strengths. In all cases, the elastic modulus with 0.2% fiber content is the highest for both the matrix strengths, similar to previous findings [6]. The lower the matrix strength, the more obvious the effect of the fiber is on the elastic modulus of the FRC [18]. The increase of the elastic modulus indicates that the ability of concrete to bear the elastic deformation of the load is reduced, which is beneficial to the non-destructive instability of the structure without causing excessive elastic deformation under load.
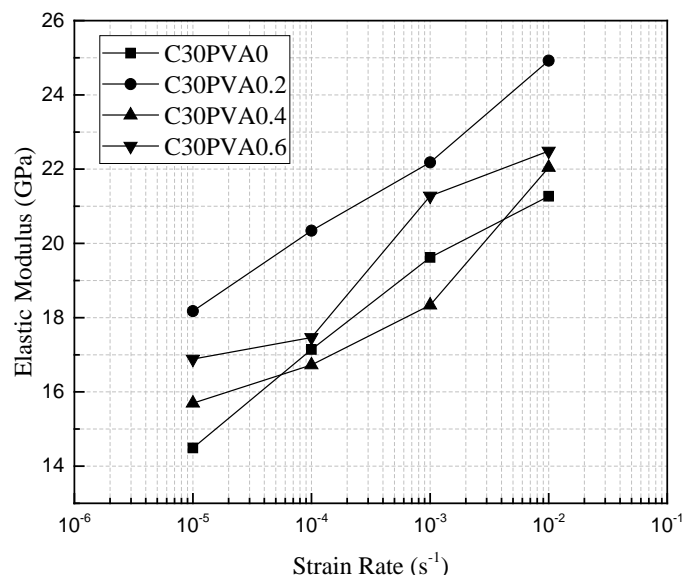
Figure 10. Elastic modulus of FRC (C30).
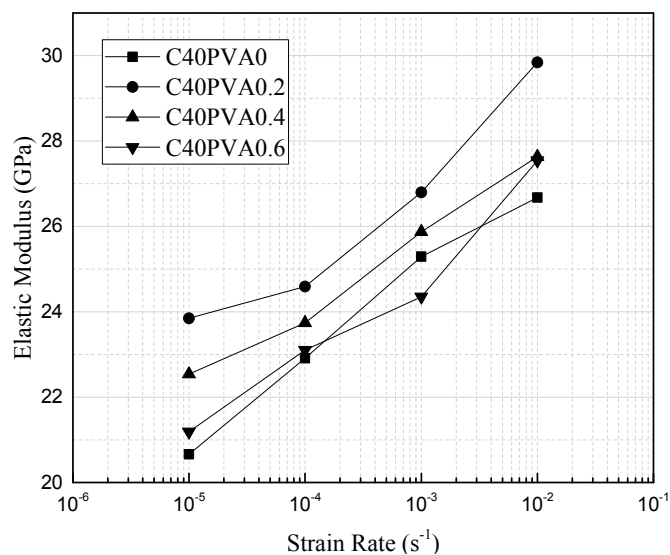
Figure 11. Elastic modulus of FRC (C40).

The peak strain of fiber concrete at different strain rates is shown in Figures 12 and 13. The peak strain here refers to the strain corresponding to the peak stress. Contrary to the trends of the strength and elastic modulus, the peak strain of concrete decreases with an increase of strain rate. The peak strain of the fiber concrete can be enhanced under each strain rate compared with plain concrete, indicating

that the addition of the fiber can improve the ability of the concrete to bear the deformation [15]. In fiber concrete, the peak strain with 0.2% fiber content is smaller than that with the other two fiber content levels, which is directly related to the maximum elastic modulus of concrete with 0.2% content.
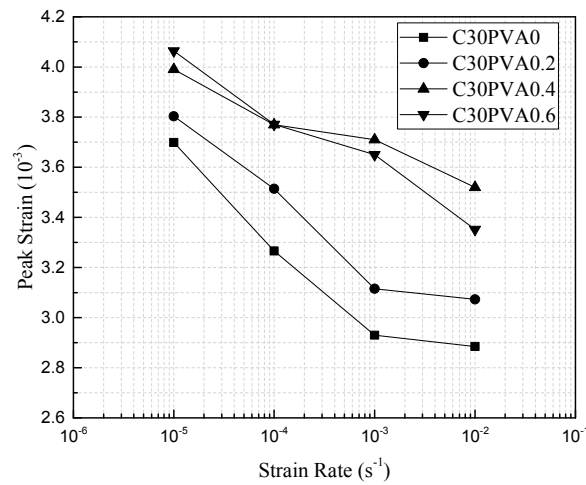
Figure 12. Peak strain of FRC (C30).
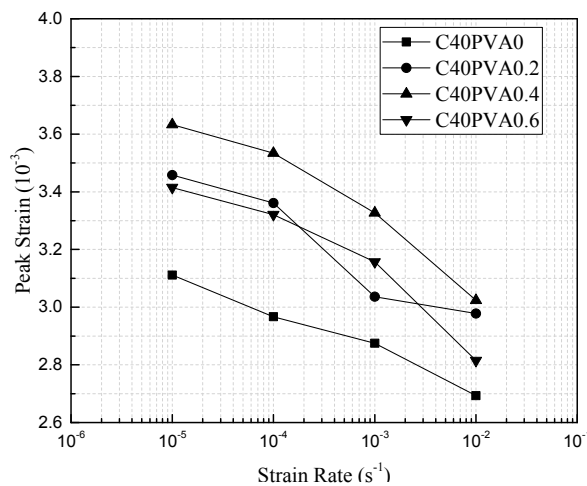
Figure 13. Peak strain of FRC (C40).

3.4. Deformation Characteristics

The typical stress–strain curves of concrete with two matrix strengths at different loading strain rates are shown in Figure 14. For the two kinds of plain concrete, the brittle characteristics of concrete became more obvious with increasing strain rate, which has been confirmed in the literature [27]. When the strain rate reaches $10^{-2}\,\text{s}^{-1}$, the failure modes have characteristics of brittle fracture, with the stress–strain curve showing a cliff-like landing. The addition of PVA can significantly improve the post-peak mechanical properties of concrete, showing a significant reduction in the drop rate per unit of time after undergoing peak stress. The stress and strain curves are smoother, indicating that the properties of the concrete change from brittle to ductile, which is of great significance in improving the seismic performance of concrete [12]. From the analysis of the typical stress and strain curves, it is found that the addition of PVA has little effect on the curve at the upward section, while showing a certain effect at the downward section. With the increase in the content of PVA, the descending rate gradually slows down at the downward section of the curve, indicating that PVA has a significant effect in improving toughness of fiber concrete [20,21]. For all types of concrete, the slopes of the stress–strain curve at the downward section increase gradually with the increase of strain rate, showing

that the bridging effect of the fiber on the concrete decreases. At this point, the loading rate plays a greater role in the failure behavior of the concrete.
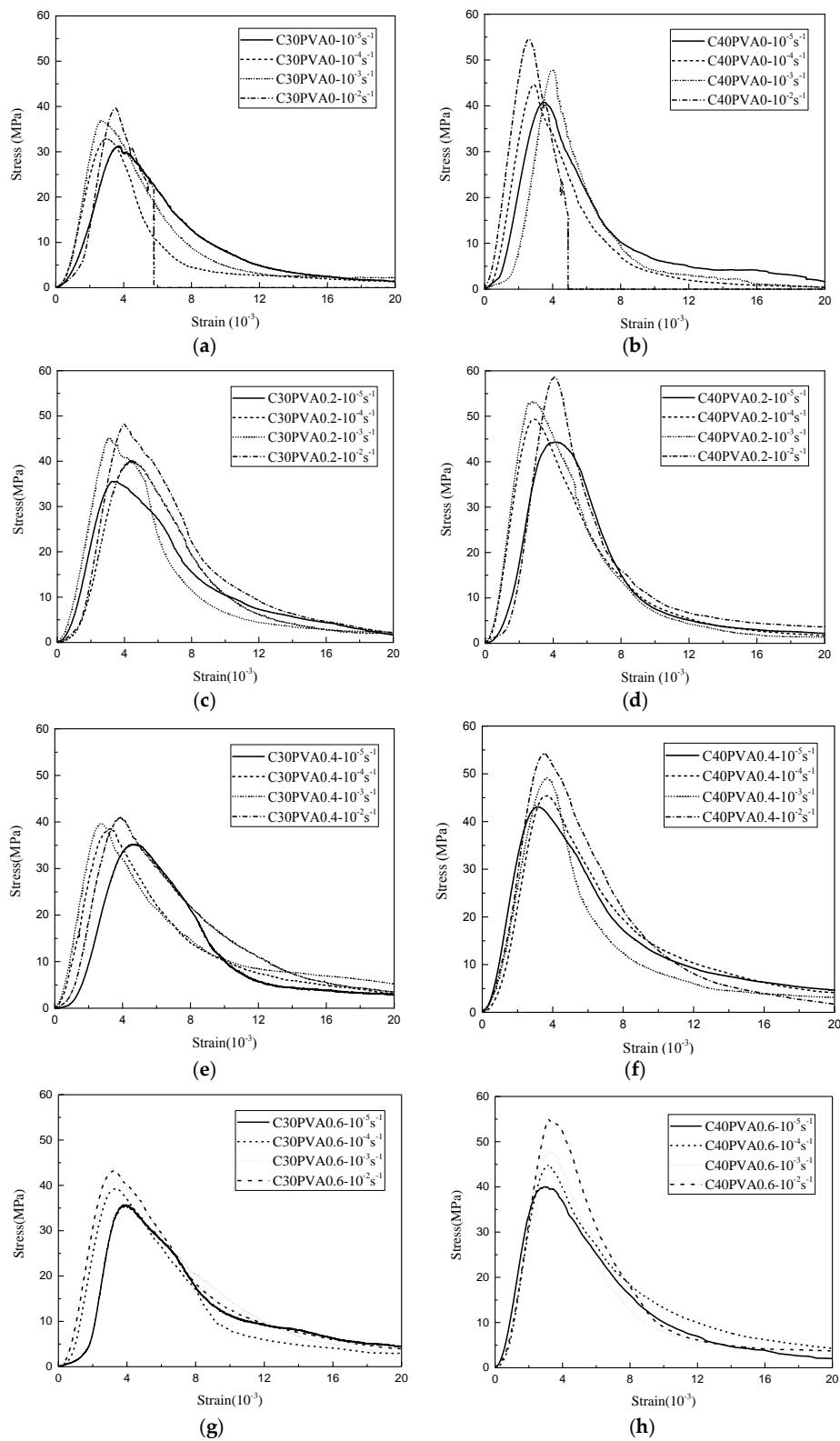
Figure 14. Typical stress–strain curve under different strain rates for (**a**) C30PVA0, (**b**) C40PVA0, (**c**) C30PVA0.2, (**d**) C40PVA0.2, (**e**) C30PVA0.4, (**f**) C40PVA0.4, (**g**) C30PVA0.6, and (**h**) C40PVA0.6.

Another aspect of the change in the post-peak mechanical properties is the residual strength and the failure mode. As shown in Figures 15 and 16, the two matrix strengths of plain concrete appear to undergo the phenomena of fall-block and caving after destruction. When the concrete block is made into a bulk, the residual strength is nearly zero. However, when the fiber concrete is crushed, the evenly distributed fibers begin to bear the load. Due to the bridging effect of the fiber, the concrete structure can maintain a relatively complete form with a number of small cracks on the surface, and the residual strength remains at approximately 3–5 MPa without brittle damage, unlike the collapse of plain concrete.

Figure 15. Typical failure modes of plain concrete under a dynamic load.

Figure 16. Typical failure modes of FRC under a dynamic load.

Therefore, the deformation characteristics of fiber concrete are different from those of plain concrete. The addition of fiber can improve the brittle properties of the concrete, including the fall-block and collapse of the concrete, the obvious decrease of the drop rate per unit time after undergoing peak stress, and the residual strength [27]. The stress–strain curves of concrete with different fiber contents are similar, and the deformation behavior of concrete at a high strain rate is more brittle than that at a low strain rate. The reinforcing effect of fiber on the mechanical properties of concrete is different for the two matrix strengths. The concrete material with low matrix strength is more ductile than the one with a higher matrix strength. The same trend is evident with the reinforcing effect of fiber improving the uniaxial compressive strength [18,26].

3.5. Toughness Index

In the evaluation of the post-peak mechanical properties of concrete, the use of the ductility index-peak strain to reflect the toughness of the material has a certain one-sidedness. Due to the large dispersion of concrete materials, there may be some errors in the peak strain of the experiment results;

hence, the use of a non-dimensional relative index to describe the toughness of the material is more reasonable. According to the method of defining the toughness of steel FRC in the literature [32,33], the formula for the toughness index can be defined for PVA-reinforced concrete as follows:

$$\eta = \frac{W_f}{W_e} \qquad (5)$$

where W_f is the area of OCD, which is defined the area surrounded by the limit strain of $20 \times E^{-3}$ in this paper; W_e is the elasticity energy consumed by concrete materials, which is defined by the area of OAB at the strain relative to $0.85*f_c$; and f_c is the peak stress. A detailed diagram is shown in Figure 17.
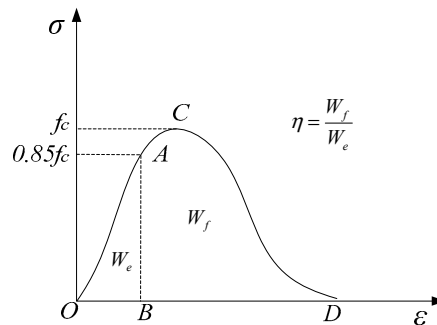
Figure 17. Diagram of the toughness index of concrete.

The above formula does not only account for both the elastic energy absorbed during the elastic phase and the plastic energy absorbed during the plastic phase of the fiber concrete, but also eliminates the energy calculation error caused by the dispersion of the concrete, which is reasonable for describing the toughness of the concrete [32]. The calculated results of the toughness indices according to the formula are shown in Table 4 and Figures 18 and 19 below.

Table 4. Calculated results of toughness index for FRC at different strain rates.

Type	Strain Rate (s^{-1})	W_f (J/m³)	W_e (J/m³)	Toughness Index
C30PVA0	10^{-5}	201.21	29.02	6.93
C30PVA0	10^{-4}	157.87	25.06	6.30
C30PVA0	10^{-3}	160.90	29.24	5.50
C30PVA0	10^{-2}	112.61	28.41	3.96
C30PVA0.2	10^{-5}	237.59	28.59	8.31
C30PVA0.2	10^{-4}	203.66	28.95	7.03
C30PVA0.2	10^{-3}	252.82	40.15	6.30
C30PVA0.2	10^{-2}	244.93	50.11	4.89
C30PVA0.4	10^{-5}	286.49	29.64	9.66
C30PVA0.4	10^{-4}	288.44	34.27	8.42
C30PVA0.4	10^{-3}	259.54	34.39	7.60
C30PVA0.4	10^{-2}	233.84	36.57	6.39
C30PVA0.6	10^{-5}	266.11	25.28	10.53
C30PVA0.6	10^{-4}	317.60	35.56	8.93
C30PVA0.6	10^{-3}	263.17	31.09	8.47
C30PVA0.6	10^{-2}	259.54	34.79	7.46
C40PVA0	10^{-5}	198.86	30.50	6.52
C40PVA0	10^{-4}	200.75	35.28	5.69
C40PVA0	10^{-3}	190.13	38.66	4.92
C40PVA0	10^{-2}	163.00	44.82	3.64
C40PVA0.2	10^{-5}	269.46	35.58	7.57
C40PVA0.2	10^{-4}	297.19	41.69	7.13
C40PVA0.2	10^{-3}	327.58	47.43	6.91
C40PVA0.2	10^{-2}	298.17	52.14	5.72

Table 4. *Cont.*

Type	Strain Rate (s^{-1})	W_f (J/m^3)	W_e (J/m^3)	Toughness Index
C40PVA0.4	10^{-5}	332.30	34.11	9.74
C40PVA0.4	10^{-4}	320.76	37.03	8.66
C40PVA0.4	10^{-3}	312.84	47.58	6.58
C40PVA0.4	10^{-2}	270.63	51.37	5.27
C40PVA0.6	10^{-5}	362.71	35.42	10.24
C40PVA0.6	10^{-4}	351.34	37.54	9.36
C40PVA0.6	10^{-3}	347.59	41.10	8.46
C40PVA0.6	10^{-2}	338.79	47.57	7.12

Note: W_f and W_e in the table are averages of three experimental results.
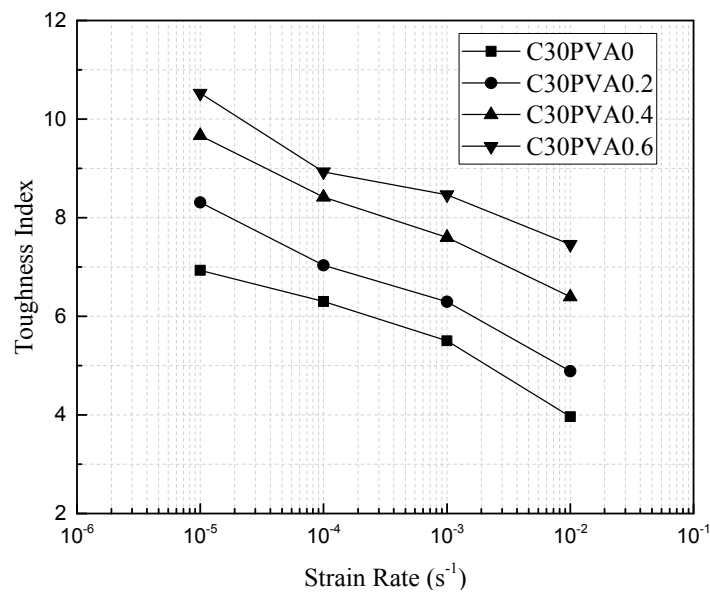
Figure 18. Toughness index of FRC (C30).
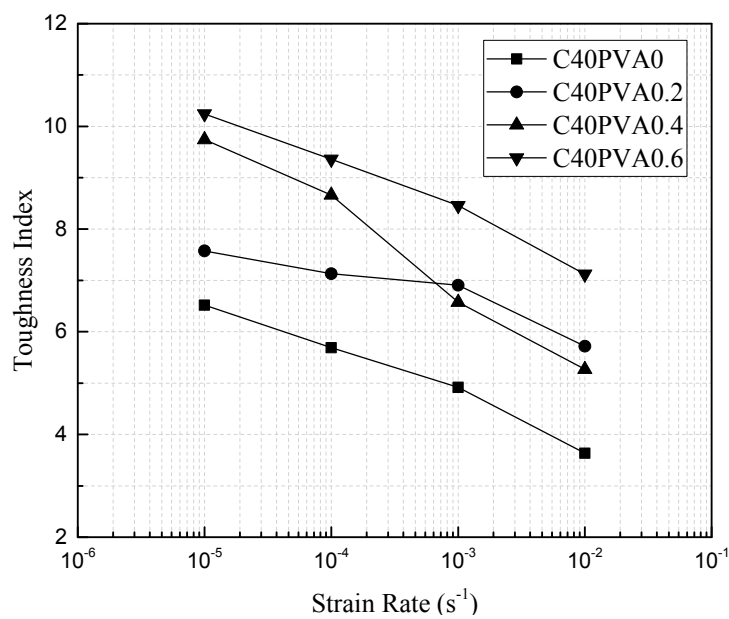
Figure 19. Toughness index of FRC (C40).

The results show that the toughness index of FRC with two matrix strengths decreases with the increase of the strain rate, and concrete material is more brittle at a high strain rate [27]. It can be seen

from Table 4 that the elastic strain energy absorbed by the FRC increases with the increase of the strain rate. The increase of the strain rate leads to the increase of the strength and elastic modulus of the concrete. There is a corresponding increase in the area surrounded by the elastic phase of the concrete stress–strain curve, indicating that the elastic strain energy of the concrete increased.

The addition of PVA can significantly enhance the toughness of concrete. In the quasi-static state (i.e., a strain rate of 10^{-5} s^{-1}), the toughness indices of FRC (C30) with 0.2, 0.4, and 0.6% content are increased by 19.9, 39.4, and 51.8%, respectively, compared to those of the plain concrete. The values are 16.2, 49.4, and 57.1%, respectively, for C40. The enhancement effect of the fiber on the concrete toughness is more obvious with the increase of fiber content. However, at a high strain rate (i.e., 10^{-2} s^{-1}), the toughness index of FRC (C30) is increased by 23.3, 61.3, and 88.2%, respectively, and the values increased 57.3, 44.9, and 95.6%, respectively, for C40. The improvement of the strain rate will lead to a decrease in the toughness index to a certain extent. However, the toughness index will be less reduced compared to the decrease in plain concrete, which shows that the toughness of the concrete with PVA decreases more smoothly with increases of the strain rate compared to plain concrete. These results illustrate that the toughness of FRC is better than that of plain concrete under the strain rate range of seismic load [20]. This is of great significance to the application of FRC in seismic design. Considering the effect of the fiber on the compressive strength, splitting strength, elastic modulus, and peak strain of concrete, as well as the cost factors and dispersion technology of the fiber, the concrete with a 0.2% PVA content is recommended for actual applications, as it can meet the engineering requirements.

4. Conclusions

In order to investigate the dynamic mechanical properties of FRC with PVA on strain rates corresponding to seismic loads (i.e., 10^{-5}, 10^{-4}, 10^{-3}, and 10^{-2} s^{-1}), the dynamic compression and splitting tensile mechanics experiment for two kinds of matrix strengths (i.e., C30 and C40) with four kinds of fiber volume contents (i.e., 0, 0.2, 0.4, and 0.6%) were carried out by using the RMT-201 rock and concrete mechanics experiment system. The physical and mechanical properties were obtained, and the following conclusions can be drawn.

(1) PVA has some enhancement and improvement effects on the concrete, mainly regarding the improvement of the compressive strength, splitting tensile strength, the toughness index, and the post-peak mechanical properties of the stress and strain curves at the descending stage. The addition of PVA can also significantly improve the failure behavior of the concrete, which changes from the fall-block and caving of plain concrete to a relatively complete form of FRC with a residual strength of 3–5 MPa. The enhancing effect of PVA on the concrete differs for two matrix strengths. The lower the matrix strength, the more obvious the reinforcing effect of the fiber is on the concrete.

(2) PVA FRC is a rate-sensitive material similar to plain concrete. The uniaxial compressive strength, splitting tensile strength, and elastic modulus of concrete increase with increasing strain rate, while the peak strain of concrete decreases, indicating that the FRC under a high strain rate is more brittle than that under a low strain rate.

(3) The PVA FRC with a 0.2% volume content has greater advantages than the other two kinds of fiber concrete in improving concrete's mechanical properties. Considering cost factors and construction convenience, concrete with a 0.2% PVA content is recommended in engineering applications.

Concrete workability should be guaranteed. Moreover, the durability issue should be deeply analyzed. In this work, to highlight the influence of strain rates on dynamic mechanical properties, these two parts were ignored. However, at a wider level, further research is also required.

Author Contributions: W.Y.: experimental tests and writing-original draft preparation; S.W.: experimental tests and discussion of the results; Z.W.: elaboration data and discussion of the results; T.X.: discussion of the results and writing-review & editing.

Conflicts of Interest: The authors declare no conflicts of interest.

References

1. Dong, J.F.; Wang, Q.Y.; Guan, Z.W. Material properties of basalt fibre reinforced concrete made with recycled earthquake waste. *Constr. Build. Mater.* **2017**, *130*, 241–251. [CrossRef]

2. Richardson, A.; Coventry, K. Dovetailed and hybrid synthetic fibre concrete–impact, toughness and strength performance. *Constr. Build. Mater.* **2015**, *78*, 439–449. [CrossRef]

3. Su, H.; Xu, J. Dynamic compressive behavior of ceramic fiber reinforced concrete under impact load. *Constr. Build. Mater.* **2013**, *45*, 306–313. [CrossRef]

4. Yan, Z.; Zhu, H.; Ju, J.W. Behavior of reinforced concrete and steel fiber reinforced concrete shield TBM tunnel linings exposed to high temperatures. *Constr. Build. Mater.* **2013**, *38*, 610–618. [CrossRef]

5. Asokan, P.; Osmani, M.; Price, A.D.F. Assessing the recycling potential of glass fibre reinforced plastic waste in concrete and cement composites. *J. Clean. Prod.* **2009**, *17*, 821–829. [CrossRef]

6. Song, P.S.; Hwang, S. Mechanical properties of high-strength steel fiber-reinforced concrete. *Constr. Build. Mater.* **2004**, *18*, 669–673. [CrossRef]

7. Yazici, Ş.; İnan, G.; Tabak, V. Effect of aspect ratio and volume fraction of steel fiber on the mechanical properties of SFRC. *Constr. Build. Mater.* **2007**, *21*, 1250–1253. [CrossRef]

8. Vajje, S.; Krishnamurthy, N.R. Study on addition of the natural fibers into concrete. *Int. J. Sci. Technol. Res.* **2013**, *2*, 213–218.

9. Sivaraja, M.; Velmani, N.; Pillai, M.S. Study on durability of natural fibre concrete composites using mechanical strength and microstructural properties. *Bull. Mater. Sci.* **2010**, *33*, 719–729. [CrossRef]

10. Agopyan, V.; Savastano, H., Jr.; John, V.M.; Cincotto, M.A. Developments on vegetable fibre–cement based materials in São Paulo, Brazil: An overview. *Cem. Concr. Compos.* **2005**, *27*, 527–536. [CrossRef]

11. Ali, M.; Liu, A.; Sou, H.; Chouw, N. Mechanical and dynamic properties of coconut fibre reinforced concrete. *Constr. Build. Mater.* **2012**, *30*, 814–825. [CrossRef]

12. Shafiq, N.; Ayub, T.; Khan, S.U. Investigating the performance of PVA and basalt fibre reinforced beams subjected to flexural action. *Compos. Struct.* **2016**, *153*, 30–41. [CrossRef]

13. Grote, D.L.; Park, S.W.; Zhou, M. Dynamic behavior of concrete at high strain rates and pressures: I. experimental characterization. *Int. J. Impact Eng.* **2001**, *25*, 869–886. [CrossRef]

14. Malvar, L.J.; Ross, C.A. Review of strain rate effects for concrete in tension. *ACI Mater. J.* **1998**, *95*, 735–739.

15. Soufeiani, L.; Raman, S.N.; Jumaat, M.Z.B.; Alengaram, U.J.; Ghadyani, G.; Mendis, P. Influences of the volume fraction and shape of steel fibers on fiber-reinforced concrete subjected to dynamic loading—A review. *Eng. Struct.* **2016**, *124*, 405–417. [CrossRef]

16. Abrams, D.A. Effect of rate of application of load on the compressive strength of concrete. *Proc. ASTM* **1917**, *17*, 364–377.

17. Cook, D.J.; Pama, R.P.; Weerasingle, H. Coir fibre reinforced cement as a low cost roofing material. *Build. Environ.* **1978**, *13*, 193–198. [CrossRef]

18. Zhang, X.X.; Abd Elazim, A.M.; Ruiz, G.; Yu, R.C. Fracture behaviour of steel fibre-reinforced concrete at a wide range of loading rates. *Int. J. Impact Eng.* **2014**, *71*, 89–96. [CrossRef]

19. Jiang, C.; Fan, K.; Wu, F.; Chen, D. Experimental study on the mechanical properties and microstructure of chopped basalt fibre reinforced concrete. *Mater. Des.* **2014**, *58*, 187–193. [CrossRef]

20. Deng, Z. *High Performance Synthetic Fiber Concrete*; Science Press: Beijing, China, 2003.

21. Holschemacher, K.; Höer, S. Influence of PVA fibers on load carrying capacity of concrete with coarse aggregates. In Proceedings of the 7th International RILEM Symposium on Fibre Reinforced Concrete: Design and Applications, Chennai, India, 17–19 September 2008; pp. 219–229.

22. Tosun-Felekoğlu, K.; Felekoğlu, B.; Ranade, R.; Lee, B.Y.; Li, V.C. The role of flaw size and fiber distribution on tensile ductility of PVA-ECC. *Compos. Part B Eng.* **2014**, *56*, 536–545. [CrossRef]

23. Suryanto, B.; Maekawa, K.; Nagai, K. Predicting the Creep Strain of PVA-ECC at High Stress Levels based on the Evolution of Plasticity and Damage. *J. Adv. Concr. Technol.* **2013**, *11*, 35–48. [CrossRef]

24. Banthia, N.; Mindess, S.; Trottier, J.F. Impact resistance of steel fiber reinforced concrete. *ACI Mater. J.* **1996**, *93*, 472–479.

25. China Academy of Building Research (CABR). *JGJ 55-2011: Specification for Mix Proportion Design of Ordinary Concrete*; China Architecture Building Press: Beijing, China, 2011.

26. National Standards of the People's Republic of China. *JG/T472-2015: Steel Fiber Reinforced Concrete*; Standards Press of China: Beijing, China, 2015.

27. Zhang, Y. *Experimental Study of the Mechanical Properties of Concrete under Different Strain Rates*; Beijing University of Technology: Beijing, China, 2012.

28. Mihashi, H.; Wittmann, F.H. Stochastic approach to study the influence of rate of loading on strength of concrete. *HERON* **1980**, *25*, 1–54.

29. Fib Model Code. *Fib Model Code for Concrete Structures 2010*; Ernst Sohn: Berlin, Germany, 2010.

30. Wu, S.; Chen, X.; Zhou, J. Tensile strength of concrete under static and intermediate strain rates: Correlated results from different testing methods. *Nucl. Eng. Des.* **2012**, *250*, 173–183. [CrossRef]

31. Shah, S.P. Experimental methods for determining fracture process zone and fracture parameters. *Eng. Fract. Mech.* **1990**, *35*, 3–14. [CrossRef]

32. Zhang, H.; Gao, Y.; Li, F. Experimental study on dynamic properties and constitutive model of polypropylene fiber concrete under high strain rate. *J. Central South Univ. (Sci. Technol.)* **2013**, *44*, 3464–3473.

33. Yi, C.; Fan, Y.; Zhu, H.; Wang, J.Q. Research on fatigue damage of concrete under uniaxial compression on the basis of toughness. *Eng. Mech.* **2010**, *27*, 113–119.